The structural and optical characterizations of tetraphenylporphyrin thin films

M.M. Makhlouf [a,b,*], A. El-Denglawey [a,c], H.M. Zeyada [b], M.M. El-Nahass [d]

[a] Physics Department, Faculty of Applied Medical Science at Turabah branch, Taif University, Turabah, 21995, Saudi Arabia
[b] Department of Physics, Faculty of Science at New Damietta, Damietta University, New Damietta 34517, Egypt
[c] Physics Department, Faculty of Science, South Valley University, Qena 83523, Egypt
[d] Physics Department, Faculty of Education, Ain Shams University, Cairo, Egypt

ARTICLE INFO

ABSTRACT

X-rays diffraction and scanning electron microscope were used to investigate the structural properties of tetraphenylporphyrin, TPP, which is polycrystalline in a synthesized condition. It turns to amorphous structure upon thermal deposition. Annealing temperature ranging from 295 to 473 K does not influence the amorphous structure of films. The optical properties of TPP were investigated using spectro-photometric measurements of the transmittance and reflectance at normal incidence in the wavelength range of 200–2200 nm. The absorption spectra were recorded in UV–visible region of spectra for the as-deposited and annealed samples show different absorption bands, namely four bands labeled as Q-band in visible region of spectra and a more intense band termed as the Soret band in near UV region of spectra. The Soret band shows its splitting (Davydov splitting). Two other bands labeled N and M appear in UV region. The film thickness has no influence on optical properties of films while annealing temperatures have a slight influence on optical properties of TPP films. The type of optical transition in as deposited and annealed conditions of films was found to be indirect allowed band-gap. Both fundamental and onset energy gap decreases upon annealing.

1. Introduction

Porphyrins are one of the most promising candidates for ordered organic semiconductors, as these systems possess many advantages such as semi-conductivity and the ability to turn from photoconductivity energy to electrical and chemical energy. This is because the porphyrin skeleton has an extended π-conjugation system that results in a wide range of wavelengths for light absorption. Porphyrins have also the advantage of being very stable (chemically and thermally) and an excellent film growth which results successfully in fabricating thin film resistors, capacitors and solar cell devices. These properties make porphyrin highly useful in fabricating electro-luminescent devices [1], photonic devices [2], solar energy conversion devices [3], photodynamic therapy and diagnosis of cancer using laser excitation [4], photochromic recording medium [5], catalysis [6], photo-electro-chemical cell [7], opto-electronic device fabrication [8] and gas sensors [9].

The basic structure of porphyrin consists of four pyrrolic subunits linked by four methane bridges. The porphyrin skeleton has an extended π-conjugation system with 18-π electrons leading to a wide range of wavelengths for light absorption.

Tetraphenylporphyrin, TPP, is non-metalloporphyrin derivative that has polymorphic crystal structures, such as triclinic [10], tetragonal [11] and monoclinic [12] forms. The TPP is centrosymmetrical with two independent pyrrole and phenyl groups as shown in Fig. 1. The absorption spectra of TPP films showed different bands depending on the method of its preparation [13–15]. The optical properties of two tetraphenylporphyrin derivatives based on tetra(4-aminosulphenyl) phenylporphyrin were examined [13]. These porphyrins can exist in both free-base and dication states with their Soret absorption bands occurring near 420 nm and 440 nm, respectively. Floating monolayers can show the occurrence of a new state characterized by two additional bands near 490 and 700 nm. The formation of this unknown state is dependent on both the sub-phase pH and the area occupied per monomer unit at the air–water interface. The absorption spectra of TPP in nematic liquid crystal have been studied [14], and spectrum shows characteristic Soret band in the blue region (400–500) nm and four small bands in the Q-band region (500–650) nm, similar absorption spectra have been obtained for the purple color of the TPP solution [15].

* Corresponding author at: Physics Department, Faculty of Applied Medical Science at Turabah branch, Taif University, Turabah 21995, Saudi Arabia. Tel.: +20 572700066, mobile: +966 547952264.
E-mail addresses: m_makhlof@hotmail.com, m.m.makhlouf@hotmail.com (M.M. Makhlouf).
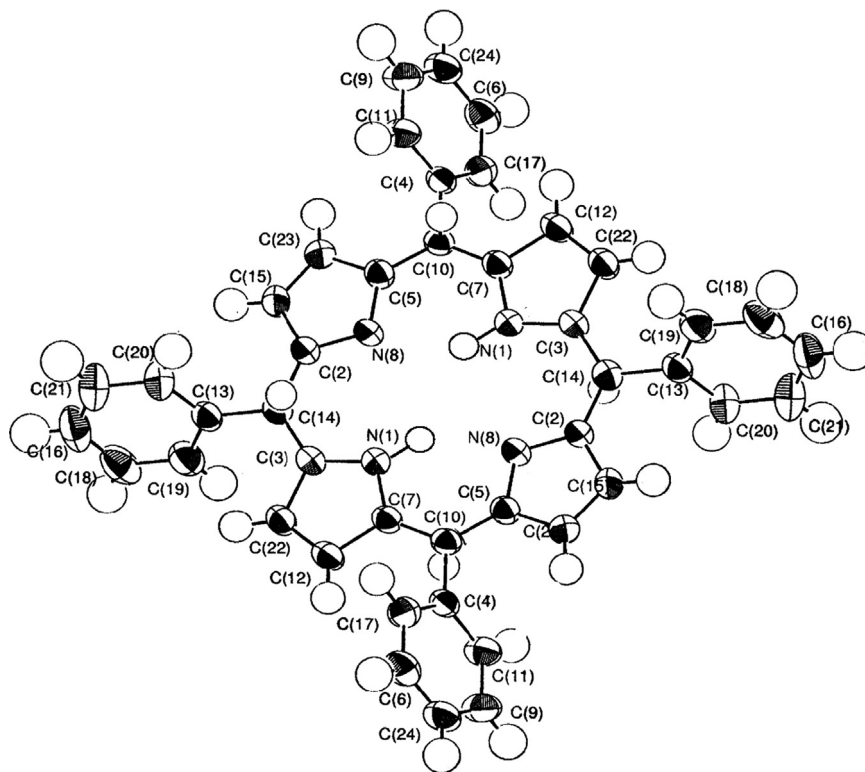
Fig. 1. Skeleton view for TPP molecular structure.

The experimental and theoretical investigations of electronic absorption spectrum for the TPP molecule in the wavelength range of 300–600 nm were carried out [16]. Comparison of experimental band positions and their intensities with the values calculated with TDDFT/(B3LYP, CAMB3LYP, M06-2X) in the framework of the PCM solution model. The results showed the efficiency of the method for description of absorption spectra for tetraphenylpor-phyrin derivatives both for the gas phase and for ethanol solution.

The first comprehensive measurement of the occupied and unoccupied electronic structure of the organic semiconductor copper tetraphenylporphyrin, CuTPP, was undertaken using X-ray photoemission spectroscopy, soft X-ray emission spectroscopy and soft X-ray absorption spectroscopy [17]. The measured electronic structure was compared to the results of a DFT calculation. The element specific partial density of states for C and N were measured and excellent agreement obtained with the calculated electronic structure.

Scrocco [18] reported specific information on the energy level diagram and on the energy gap of TPP and its Ni derivative that have been obtained by means of electron energy loss spectroscopy (EELS) and X-ray photoelectron spectroscopy (XPS) techniques. A good estimate of the energy gap in the species has been discussed in connection with their semiconducting properties. Comparison of the free metal TPP and its derivative emphasizes the importance of the metal Ni 3d levels in the conduction processes.

Composite films were produced by successive vapor-deposition of nylon-11 and porphyrin compounds, TPP and ZnTPP [19]. The composite films were characterized by X-ray diffraction, scanning electron microscopy and visible spectroscopy. Naylon-11 was vapor-deposited on a glass plate to produce a thin film with thickness 1 μm, and the TPP particles were dispersed into the interior of the nylon-11, the morphology and the dispersion behavior observed in the TPP/nylon-11 films and they found that they are dependent on the chemical characteristics of the por-phyrin compounds. These films showed a transformation of structure morphology by heat treatment at 120 C°. The optical absorption spectrum for TPP/nylon-11 and ZnTPP/nylon-11 films were measured. Visible absorption spectra of the samples show a very sharp absorption band at 420 nm, and it was assigned to be the Soret band of TPP. Such a sharp Soret band was generally observed in a solution of TPP [20].

Spectral characteristics of TPP have been studied in acetonitrile medium in the presence of zinc perchlorate [21]. Absorption spectral studies indicate the formation of a new complex between zinc ion and the porphyrin moiety in the ground state as distinguished from the characteristics of metalo (zinc) porphyrin compound. The TPP can behave as a new ratiometric fluorescent sensor. This fluorescence modulation of TPP should be applicable to dual-wavelength measurement of various biomolecules or enzyme activities. The fluorescence emission of tetraphenylpor-phyrin at 651 nm bands decreases while that at 605 nm increases upon zinc ion interaction in acetonitrile.

To our knowledge absorption spectra, optical properties and spectral features of TPP thin films prepared by thermal evapora-tion technique have not been investigated yet. The aim of the present work is to study the influence of some environmental conditions (film thickness and annealing temperature) on the structural, optical properties and spectral features of thermally-evaporated TPP thin films. Application of TPP in any of the above devices will certainly be provided as thin films. The effect of annealing temperature on the optical parameters was calculated.

2. Experimental details

A dark violet crystalline powder of tetraphenylporphyrin, TPP, was purchased from Aldrich Chem. Co., and was used as received without any further purification. TPP thin films were sublimated by conventional thermal evaporation technique using high vacuum coating system (Model 306A, Edward Co., England).

The films were deposited onto clean glass substrates for X-ray diffraction (XRD) analysis and onto optical flat quartz substrates

for optical measurements. The quartz substrates were carefully cleaned by putting them in chromic acid for 15 min and then rinsed by deionized water. The material was sublimated from a quartz crucible source heated by a tungsten coil in a vacuum of 10^{-4} Pa. The rate of deposition was controlled at 2.5 nm/sec using a quartz crystal thickness monitor (Model FTM4, Edward Co., England). The thickness was also monitored by using the same thickness monitor. A shutter, fixed near to the substrate, was used to avoid any probable contamination on the substrates in the initial stage of evaporation process and to control the thickness of films accurately.

The structural analysis of TPP in powder form, as-deposited and annealed thin films were analyzed by XRD system (model X$^{\backslash\backslash}$ Pert Pro, Philips Co.) equipped with Cu target. The filtered Cu K$_\alpha$ radiation ($\lambda = 1.5408$ Å) was used. The X-ray tube voltage and current were 40 kV and 30 mA, respectively. TPP thin film was investigated using a ZEISS ultra-plus model field emission scanning electron microscopy.

The transmittance, $T(\lambda)$, and reflectance, $R(\lambda)$, spectra of the films were measured at normal incidence of light in spectral range 200–2200 nm using a double-beam spectrophotometer (JASCO model V-570 UV–vis–NIR), for deposited films in the thickness range of 175–735 nm. An uncertainty of 1% was given by the manufacturer for the measurements obtained by this spectrophotometer. A quartz blank substrate identical to the one used for the thin film deposition was used as a reference for the absorption scan. These measurements were also performed for the films after being annealed at 473 K for a soaking time of 2 h.

3. Method of calculation

The present model includes a monochromatic beam of light impinging on a thin film deposited on a thick transparent substrate, multiple reflections occur at the interface of the system. Assume that these reflections are coherent in the thin film and incoherent in the substrate, the absolute expressions of total measured transmittance, T, reflectance, R, and back reflectance, R', after introducing corrections resulting from the absorption and reflection of the substrate are given by [22,23]

$$T = \frac{I_{ft}}{Iq}(1 - R_q) \tag{1}$$

where I_{ft} and I_q are the intensities of light passing through the film–substrate system and reference quartz.

$$R = \left(\frac{I_{fr}}{I_q}\right)R_m \tag{2}$$

where I_{fr} and I_m are the intensities of light reflected from the sample and reference mirror reaching the detector respectively. R_m is the mirror reflectance.

$$R' = \left(\frac{I'_{ft}}{I_m}\right)R_m R_q \tag{3}$$

where I'_{ft} is the intensity of incident light on substrate system only and R_q is the reflectance of quartz substrate.

The film transmittance, T_f, film reflectance, R_f, and film back reflectance, R'_f, for a system consisting of deposited film onto semi-infinite transparent substrate of refractive index, n_s, and reflectance, R_q, are expressed as [24]

$$T = \frac{T_f(1 - R_3)}{1 - R_3 R'_f}, \tag{4}$$

$$R = R_f + \frac{T_f^2 R_3}{1 - R_3 R'_f}, \tag{5}$$

$$R' = \frac{R_3 + R'_f(1 - 2R_3)}{1 - R_3 R'_f}. \tag{6}$$

where R_f and T_f are the reflectance and transmittance of the air–film interface in the direction of incident beam, $T_f R_3$ is the first internal reflection in the substrate–air interface, $T_f R_3 R'_f$ is the second internal transmittance of film–air interface. Substituting Eqs. (6) in (4) and (5), a simple formulae for calculating film transmittance, T_f, and reflectance, R_f, are obtained as

$$T_f = T \frac{[(1 + R_q)^2 - 2R_q R']}{1 + R_q(1 - R') + R_q^2(R' - 2)}, \tag{7}$$

$$R_f = R - \left[\frac{T_f^2 R_q[1 - R_q(R' - 2)]}{(1 + R_q)^2 - 2R_q R'} \right] \tag{8}$$

To calculate the refractive index, n, and absorption index, k, of films, Soliman et al. [25] introduced a computer program comprising a modified search technique of Abélés et al. [26]. This technique is based on minimizing $|\Delta T|^2$ and $|\Delta R|^2$ simultaneously, where

$$|\Delta T|^2 = |T_{(n,k)} - T_{\exp}|^2 \tag{9}$$

$$|\Delta R|^2 = |R_{(n,k)} - R_{\exp}|^2 \tag{10}$$

where T_{exp} and R_{exp} are the experimental values of T and R measured from Eqs. (7) and (8), respectively. $T_{(n,k)}$ and $R_{(n,k)}$ are the calculated values of T and R, using Murmann's equations [27,28]. By applying such a technique [25], unique values of n and k are obtained within the desired accuracy. An optimization step-length technique follows to speed up the convergence and to shorten the run time needed to improve associated accuracy. The experimental errors were taken into account as follows: $\pm 2.2\%$ for film thickness measurements, $\pm 0.1\%$ for T_f and R_f calculations, $\pm 3\%$ for refractive index and $\pm 2.5\%$ for absorption index measurements [29].

4. Results and discussion

The single crystal and molecular structure calculations for TPP were determined with graphite monochromated MoK$_\alpha$ radiation ($\lambda = 0.711$ Å) on automatic Kappa CCD single crystal diffractometer (Enraf Nnious FR59) computer controlled system. TPP was recrystallized from a mixture of chloroform and benzene by slow evaporation of TPP saturated solution followed by drying at room temperature. The largest available crystal specimen is a prism of approximate dimensions $0.23 \times 0.21 \times 0.13$ mm^3. A survey of diffraction pattern for TPP, performed at room temperature (295 K), was showed skeleton view for TPP molecular structure as in Fig. 1. The molecular structure calculations for TPP indicated that the crystal system is triclinic and that there is only one TPP molecule per unit cell. The unit cell parameters are $a = 6.438$ Å, $b = 10.481$ Å, $c = 12.42$ Å, $\alpha = 95.9°$, $\beta = 99.3°$, $\gamma = 101.2°$, $V = 803$ Å^3 while the density is 1.274 g/cm^3.

Fig. 2 illustrates the growth of layer TPP as a deposited thin film. The SEM film morphology of TPP shows the details for the structure orientation of individual TPP molecules which agree with the molecular structure of TPP in Fig. 1.

The XRD pattern of TPP in the powder form, Fig. 3, shows many peaks with different intensities. This indicates that the material is polycrystalline. Fig. 4 shows diffraction pattern of thermally-evaporated TPP film of thickness 460 nm. The diffraction pattern exhibits broad peak around $2\theta = 23°$ indicating that the evaporated TPP thin film is amorphous, and increasing annealing temperatures up to 473 K does not affect the amorphous structure of
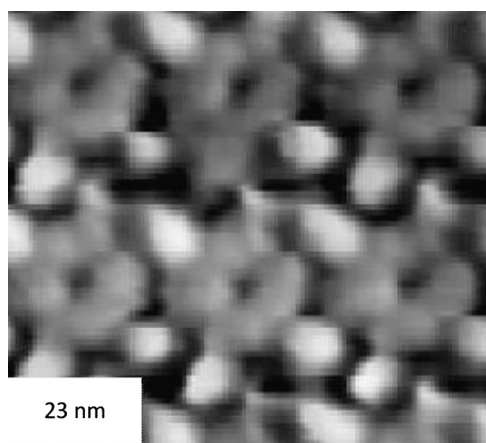
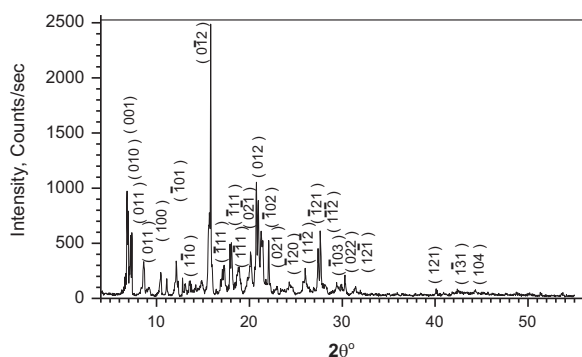**Fig. 2.** SEM image for a deposited TPP thin film.

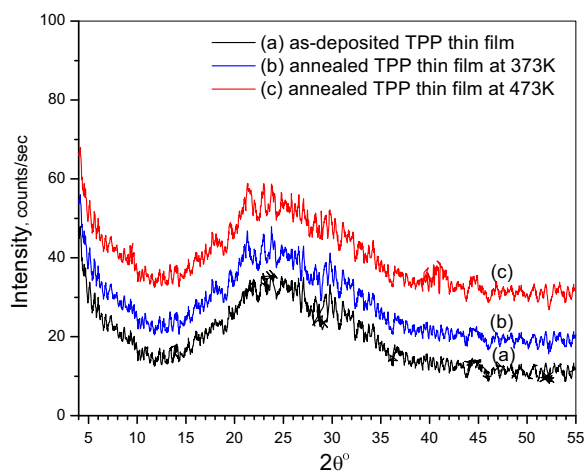**Fig. 3.** X-ray diffraction pattern of TPP in powder form.

Fig. 4. X-ray diffraction pattern of TPP thin films with thickness of 460 nm annealed at different temperatures: (a) 295 K, (b) 373 K and (c) 473 K.

evaporated TPP films, which indicates the thermal stability of TPP thin films.

Fig. 5 illustrates the absorption spectra of the as deposited and annealed TPP thin films with different thickness range 175–735 nm. Fig. 5(a) demonstrates the absorbency in both UV and visible regions of spectra for as-deposited film. The highly conjugated tetraphenylporphyrin macrocycle shows intense absorption termed Soret band that appeared in the wavelength range of 360–490 nm; such sharp Soret band was observed in solution of TPP dissolved in chloroform solvent [20]. Four additional weaker
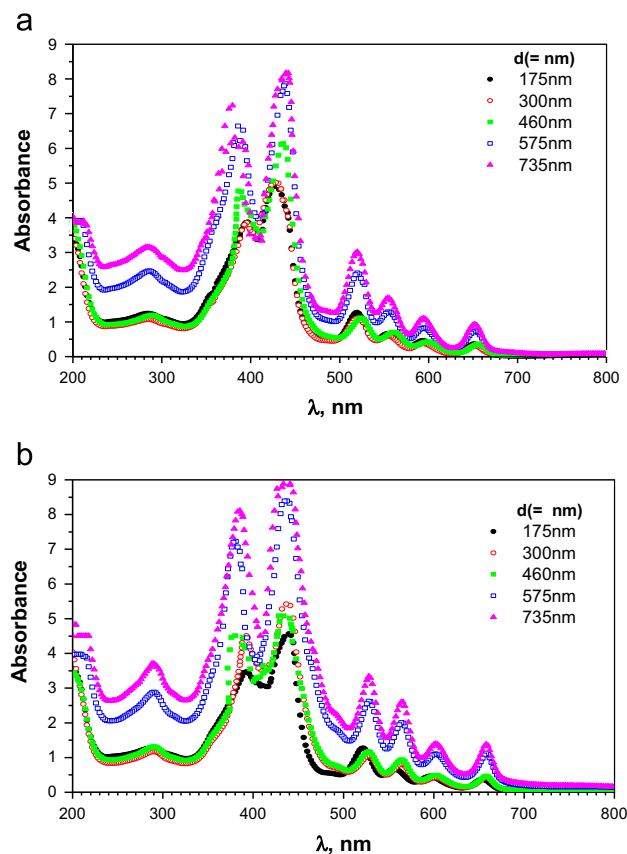

Fig. 5. The optical absorption spectrum of TPP thin films with different thickness ranged from 175 to 735 nm: (a) as-deposited films and (b) after annealing at 473 K for 2 h.

absorption peaks termed Q bands in the range of 500–720 nm were also detected. This absorption spectrum agrees with the absorption of TPP dissolved in nematic liquid crystal, which showed the Soret band in the region from 400 to 500 nm and small bands in the Q band region from 500 to 650 nm. It is shown that there is an increase in the absorption peak's intensity with increase in film thickness. It is also shown that the absorbance of films increases with increasing film thickness without changing peak position. The peaks may be generally interpreted in terms of π–π^* transition between bonding and anti-bonding molecular orbitals [30–32]. It is also noted that the bands B, N and M appear with intensities that are comparatively higher than that of Q band, which is because absorption transitions in the Q-band region have small oscillator strengths due to opposite direction of the electric dipoles and the cancellation of electric dipoles that occurs leading to low intensity in the Q bands. The interaction between two or more molecules in the unit cell of the aggregate results in two or more excitonic transitions with high transition moment and the original absorption band is split into two or more Davydov splitting [33]. The Soret band has two peaks, B_x and B_y, at 395 and 443 nm. The exciton model developed by Kasha et al. [34] predicted that the splitting or shift absorption band is caused by the interaction of localized transition dipole moments. The two absorption transitions, B_x and B_y, due to splitting in the Soret band, have high intensity because the Soret band has parallel electric dipoles [35].

Fig. 5(b) demonstrates the influence of annealing conditions on the absorbency spectrum of TPP. Annealing results in significant broadening of the Soret band and causes a slight red shift of absorption bands indicating an increase of π-conjugation due to increased planarity [36].
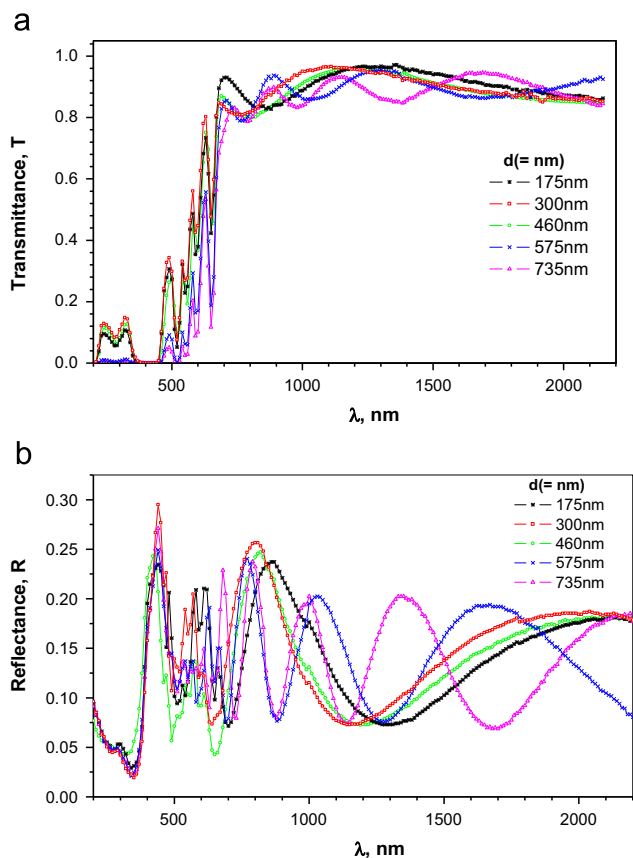
Fig. 6. Spectral distribution of transmittance and reflectance of different thickness thin films in as-deposited condition: (a) transmittance and (b) reflectance.

Fig. 7. Spectral distribution of transmittance and reflectance of different thickness thin films after annealing at 473 K for 2 h: (a) transmittance and (b) reflectance.

Yuan et al. have been studying structure characterization for several porphyrin derivatives [37]. They reported that TPP exhibits a highly ordered columnar stacking in the solid crystalline and TPP films were found to have a disordered structure [37]. This result was observed for TPP thin films as shown in Fig. 4. The amorphous morphology due to the formation of face-to-face molecular of stacking leads to formation of H-aggregates. Since the energy of an exciton on an H-aggregate will be lower than on an individual molecule in a less ordered domain in the film, H-aggregates may act as exciton traps that lead to a more amorphous morphology of the TPP film [38,39]. Kasha model [34] suggested mutual orientations for the individual molecules in a self-assembled stack and for the alignment of the stacks with respect to the substrate. This implies that the parallel orientation between assembled TPP stacks and substrate is possible, if the inter-molecular angle is $> 54°$. Therefore, π-electrons of each porphyrin molecule overlap in the columns and the Soret band becomes broader due to the $\pi-\pi^*$ electric interaction and red shift is consistent with decrease of the HOMO–LUMO gap.

The spectral behavior of $T(\lambda)$ and $R(\lambda)$ measured at normal incidence in the wavelength ranged from 200 to 2200 nm for as-deposited TPP thin films with the thickness ranging from 175 to 735 nm as presented in Fig. 6(a and b). The measurements were also performed for the same samples after being annealed at 473 K for 2 h. as shown in Fig. 7(a and b). Fig. 6(a and b) shows that the spectrum can be divided into two regions: (a) in the wavelength ranged from 200 to 700 nm, $R(\lambda) > T(\lambda)$ and their total sum is less than unity (absorbing region) in the wavelength range from 390 to 470 nm, the transmittance is zero, i.e. there is no light that transmits out of the sample and all waves of light are either absorbed or reflected. It is also observed that intensity of
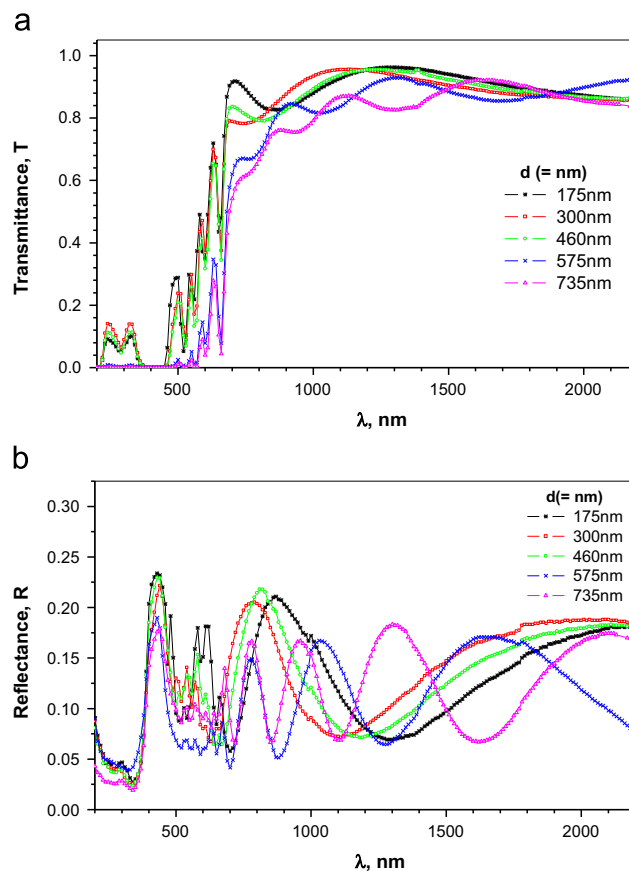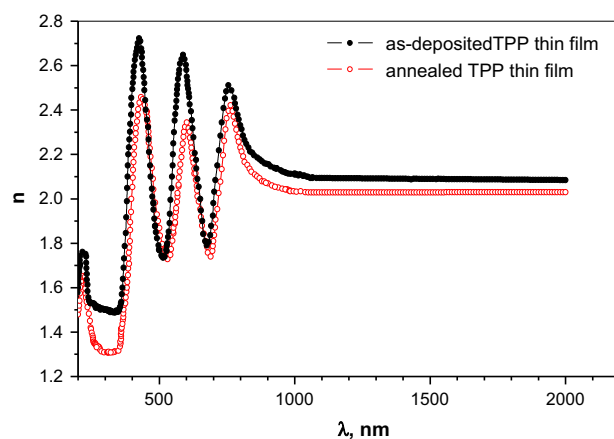

Fig. 8. The dispersion curve of the refractive index $n(\lambda)$ for TPP thin films as-deposited and annealed at 473 K for 2 h.

transmittance peaks in absorption region decreases with an increase in the film thickness. (b) At longer wavelength, $\lambda > 700$ nm, all films become transparent, $T(\lambda) \gg R(\lambda)$, and no light was scattered or absorbed as $T+R \approx 1$ (transparent region). Therefore, $k=0$ and we can calculate n only for such films. The oscillations in the values of $T(\lambda)$ and $R(\lambda)$ are a result of light interference in the considered wavelength range, we also conclude that the light is not dispersed and this indicates that the films are homogenous and optical flat. The above mentioned phenomena occur also in thin films that were annealed at 473 K for 2 h with a slight dependence on annealing temperature as it is shown in Fig. 7(a and b). This result proves that TPP films have thermal stability.
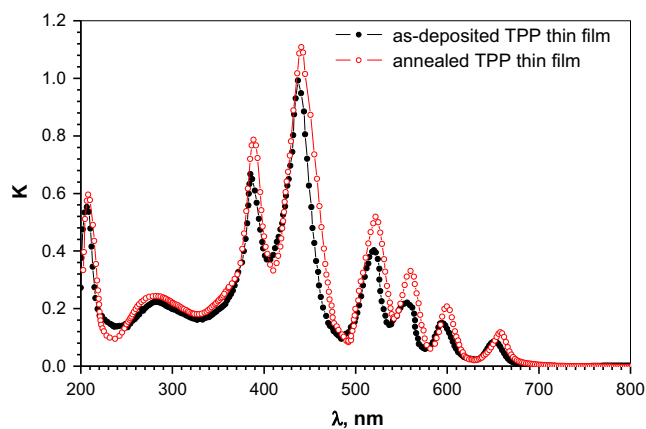
Fig. 9. The spectral distribution of the absorption index $k(\lambda)$ for TPP thin films as-deposited and annealed at 473 K for 2 h.
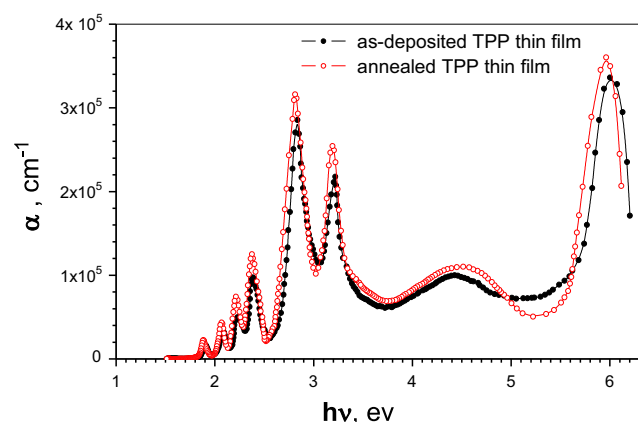

Fig. 10. The spectral behavior of the absorption coefficient α for TPP thin films as-deposited and annealed at 473 K for 2 h.

The spectral distribution of the refractive index, n, and absorption index, k, are depicted in Figs. 8 and 9. The calculations of n and k were carried out for films with different thicknesses ranging from 175 to 735 nm before and after annealing process. The calculated optical constants were found to be independent of the film thickness in the wavelength range used for measurements and within the estimated experimental errors. The dispersion curve of refractive index $n(\lambda)$ for TPP, plotted from the mean values of various film thickness in the wavelength range of 200–2200 nm and is presented in Fig. 8. It shows an anomalous dispersion in the wavelength ranged from 200 to 900 nm exhibiting four absorption peaks in the UV–visible regions. However, these are explained by using a multi-oscillator model. At a wavelength greater than 900 nm, the spectral behavior of n becomes normal dispersion, while the refractive index decreases rapidly and then the rate of decrease becomes very slow, reaching a nearly constant value at around 1200 nm. The single oscillator model is applied in the region of normal dispersion and the data are used to obtain the dielectric function and the oscillator parameters at high frequencies. The annealing process shifts the peaks slightly towards higher wavelength and reduces intensities of absorption peaks, the results of absorption index, k, depicted in Fig. 9 shows eight absorption peaks in UV–visible region. These are attributed to electronic transition across π–π^* orbitals, the peaks' intensities increase with annealing temperature and slightly shift towards higher wavelength—red shift.

The absorption coefficient, α, of TPP variation versus incident energy photon before and after annealing is illustrated in Fig. 10.

The absorption coefficient is calculated from the average absorption index as $\alpha = 4\pi k/\lambda$ and photon energy is given by $1.24/\lambda_{\mu m}$. The analysis of the absorption coefficient spectra of TPP in the range of photon energies (1.2–6.2) eV reveals the contribution from different absorption processes. The spectrum is divided into four regions: Q-band region (1.8–2.5) eV, B-band region (2.5–3.7) eV, N-band region (3.7–5.3) eV and M-band region (5.3–6.2) eV. Table 1 lists the energies of the absorption maxima present in the spectra, in UV–visible region of absorption spectrum. The highly conjugated porphyrin macrocycle shows several transition bands. The four-orbital model [31,32,35] provides a basis for quantitative estimation of the transition and changes in the electronic states of porphyrins, such model parameterizes the molecular orbital configuration that gives rise to π–π^* transitions in TPP. The two interband transitions Q and B are assigned as π–π^* type [25], from the two highest occupied molecular orbitals (HOMO) levels $1a_{1u}(\pi)$ and $4a_{2u}(\pi)$ to the first excited lowest unoccupied molecular orbital (LUMO) level $5e_g(\pi^*)$ [32,37]. The transition bands in UV region are assigned as the N band transition from HOMO level $3a_{2u}(\pi)$ to LUMO level $5e_g(\pi^*)$ and the M band transition from HOMO level $1b_{1u}(\pi)$ to LUMO $5e_g(\pi^*)$ [35,37]. The intense absorption at around 430 nm is termed Soret band. Davydov or excitonic splitting has been proposed as a mechanism for broadening excited state, the energy separation due to Davydov splitting, ΔQ, is as shown in Table 1 in the order of 0.362 eV and 0.365 eV before and after annealing respectively.

The types of transition and the value of optical energy gap can be demonstrated by Bardeen et al. equation [40] as

$$\alpha h\nu = \alpha_o(h\nu - E_g)^r \qquad (11)$$

The direct and indirect allowed–forbidden band-gaps of the TPP films may roughly be estimated by plotting the $(\alpha h\nu)^{1/r}$ versus $h\nu$ ($r=1/2$ for allowed direct, $r=2$ for allowed indirect, $r=3$ for forbidden indirect and $r=3/2$ for forbidden direct optical transitions) and extrapolating the linear region of the plot toward low energies. The dependence of $(\alpha h\nu)^{1/r}$ on photon energy ($h\nu$) for fundamental and onset gaps were discussed and plotted for different values of r, and the best fit was obtained for $r=2$ as illustrated in Fig. 11. This is characteristic behavior of indirect allowed transitions. The relation between $(\alpha h\nu)^{1/2}$ and ($h\nu$) for as-deposited films before and after annealing is linear in the region of strong absorption edge for fundamental and onset bands. The extrapolation of the straight line graphs $(\alpha h\nu)^{1/2}=0$ will give the value of the optical band gap as shown in Fig. 11. The values of indirect energy E_g^{ind} and the phonon energies E_{ph} for the films before and after annealing in the two regions are listed in Table 2. The calculated energy gap for Q-band between full and empty orbitals is 1.778 eV and this value agrees with the experimental values (1.8–1.9 eV) [31,32]. It is obvious that the energy gap decreases with increasing annealing temperature and slightly shifts towards higher wavelength that appears in spectral behavior of optical properties.

5. Conclusion

The analysis of X-ray diffractograms of TPP proved that the received powder material form polycrystalline patterns with triclinic structure. The as-deposited TPP thin films have amorphous structure. Annealing temperature does not influence amorphous structure of as-deposited films indicating that TPP films have thermal stability. The absorption spectra of thermally-evaporated free-base tetraphenyl-porphyrin consist of four Q-bands in the region 500–720 nm and an extremely intense Soret band has two peaks at 395 nm and 443 nm. Two other weak bands labeled N and M appeared at the shorter wavelengths, UV

Table 1
The absorption peak maxima of TPP for as-deposited and annealed thin films.

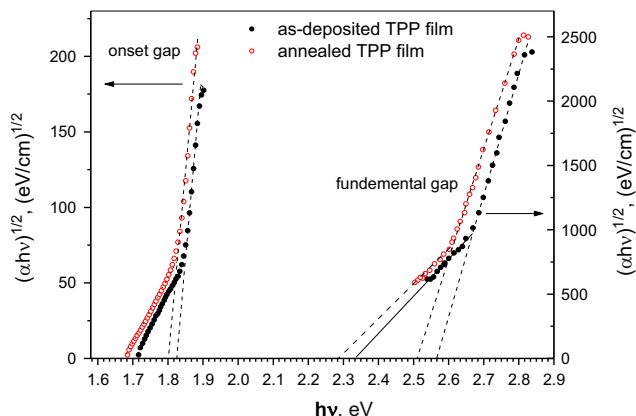| TPP bands	Visible (Q) (eV)				Soret (B) (eV)		N (eV)	M (eV)	ΔQ (eV)
As-deposited	1.88	2.08	2.227	2.388	2.838	3.201	4.419	601	0.362
Annealed	1.9	2.06	2.208	2.367	2.819	3.184	4.398	5.95	0.365

Fig. 11. Relation between $(\alpha h\nu)^{1/2}$ and photon energy $(h\nu)$ for TPP as-deposited and annealed films at 473 K for 2 h.

Table 2
Energy gaps and phonon energies of TPP for as-deposited and annealed thin films.

Compound condition	Fundamental energy gap		Onset energy gap	
	$E_g^{ind}(eV)$	$E_{ph}(meV)$	$E_g^{ind}(eV)$	$E_{ph}(meV)$
TPP as-deposited	2.45	115	1.778	58
TPP annealed	2.39	110	1.734	61

region. The optical constant n and k are independent of film thickness and are slightly dependent on annealing temperature. The type of electronic transition responsible for optical properties is an indirect allowed transition. The onset and fundamental energy gaps of as-deposited films are 1.778 eV and 2.45 eV, respectively. Annealing decreases them to 1.734 eV and 2.39 eV, respectively.

Acknowledgments

References

[1] Guolun Zhong, Jun Wu, Yonghong Wang, Rong Li, Jinbao Xu, Jianzhong Sun, Thin Solid Films 517 (11) (2009) 3340.

[2] Danuta Wróbel, Aleksandra Siejak, Przemys Law Siejak, Sol. Energy Mater. Sol. Cells 94 (3) (2010) 492.
[3] Na Xiang, Weiping Zhou, Shenghui Jiang, Lijun Deng, Yijiang Liu, Zhuo Tan, Bin Zhao, Ping Shen, Songting Tan, Sol. Energy Mater. Sol. Cells 95 (2011) 1174.
[4] Y. Chen, G. Li, R.K. Pandy, Curr. Org. Chem. 8 (2004) 1105.
[5] Javier Durantini, Gustavo Morales, Marisa Santo, Matias Funes, Edgardo N. Durantini, Fernando Fungo, Thomas Dittrich, Luis Otero, Miguel Gervaldo, Org. Electron. 13 (4) (2012) 604.
[6] Jie Li, Jianping Lei, Quanbo Wang, Peng Wang, Huangxian Ju, Electrochim. Acta 83 (30) (2012) 73.
[7] Kang Deuk Seo, Myung Jun Lee, Hae Min Song, Hong Seok Kang, Hwan Kyu Kim, Dyes Pigm. 94 (1) (2012) 143.
[8] Corrado Di Natale, Danio Salimbeni, Roberto Paolesse, Antonella Macagnano, Arnaldo D'Amico, Sens. Actuators B Chem. 65 (1–3) (2000) 220.
[9] P. Muthukumar, S.Abraham John, Sens. Actuators B Chem 159 (1) (2011) 238.
[10] E.B. Fleisher, C.K. Miller, L.R. Webb, J. Am. Chem. Soc. 86 (1964) 2342.
[11] S.J. Silvers, A. Tulinsky, J. Am. Chem. Soc. 89 (1967) 3331.
[12] M. Ashida, H. Yanagi, S. Hayashi, K. Takemoto, Acta Cryst. B47 (1991) 87.
[13] M.B. Grieve, A.J. Hadson, T. Richardson, R.A. Johnstone, A.J. Sobral, A.M. Rocha, Thin Solid Films 243 (1993) 581.
[14] D. Wrobel, J. Lukasiewicz, J. Goc, R.M. Ion, J. Mol. Struct. 450 (1998) 239.
[15] Tandrima Chaudhuri, Dibakar Goswami, Manas Banerjee, Spectrochim. Acta A 79 (2011) 131.
[16] R.R. Valiev, E.G. Ermolina, Yu.N. Kalugina, R.T. Kuznetsova, V.N. Cherepanov, Spectrochim. Acta A 87 (2012) 40.
[17] Ian Reid, Yufeng Zhang, Alex Demasi, Andrew Blueser, Louis Piper, James E. Downes, Anne Matsuura, Greg Hughes, Kevin E. Smith, Appl. Surf. Sci. 256 (2009) 720.
[18] M. Scrocco, J. Electron Spectrosc. Relat. Phenom. 60 (1992) 363.
[19] K. Sayo, S. Deki, T. Naguchi, K. Goto, Thin Solid Films 349 (1999) 276.
[20] Takuji Yutaka Harima, Paul Kodaka, Tsukasa Price, Kazuo Yamashita Eguchi, Thin Solid Films 307 (1997) 208.
[21] Tandrima Chaudhuria, Dibakar Goswami, Manas Banerjee, Spectrochim. Acta A 79 (2011) 131.
[22] L.A. Agiev, I.N. Shklyarevskii, J. Prekel Spekt 76 (1978) 380.
[23] I.N. Shklyarevski, T.I. Kornveeva, K.N. Zozula, Opt. Spectrosc. 27 (1969) 174.
[24] Y. Laaziz, A. Bennouna, N. Chahboun, A. Outzourhit, E.L. Ameziome, Thin Solid Films 372 (1966) 325.
[25] H.S. Soliman, N. EL-Kadry, O. Gamjoum, M.M. EL-Nahass, H.B. Darwish, J. Opt. 17 (2) (1988) 46.
[26] F. Abélés, M.L. Théyé, Surf. Sci. 5 (1966) 325.
[27] O.S. Heavens, G. Hass, T. Thus (Eds.), Academic Press, New York, 1964.
[28] J.M. Liddeli, Computer-Aided Technique for the Design of Mlutilayer Filters, Hilger, Bristol (1981) 118.
[29] I. Konstantiov, T. Babes, S. Kitova, Appl. Opt. 37 (19) (1998) 4260.
[30] W.R. Scheidt, Y.J. Lee, J. Struct. Bondin., (Berlin) 1 (1987) 64.
[31] A.M. Shaffer, M. Gouterman, Theor. Chim. Acta 25 (1972) 62.
[32] M. Gouterman, The Porphyrins, Academic Press, New York, 1978.
[33] A.S. Davydov, Theory of Molecular Excitons, Plenum press, New York, 1971.
[34] M. Kasha, H.H. Rawls, Ashraf El-bayoumi, Pure Appl. Chem 11 (34) (1965) 371.
[35] E.J. Baerends, G. Ricciard, A. Rosa, S.J. Van Gisbergen, Coord. Chem. 230 (2002) 5.
[36] G. Scott, L.A. Harry, Chem. Commun. (1999) 1539.
[37] Y. Yuan, B.A. Gregg, M.F. Lawrence, J. Mater. Res. 15 (11) (2000) 2494.
[38] A. Huijser, T.J. Savenije, A. Kotlewski, S.J. Picken, L.D.A. Siebbeles, Adv. Mater. 18 (2006) 2234.
[39] O.B. Locos, Synthesis and investigations of novel alkenylporphyrins and bis (porphyrins) (Ph.D. thesis), The Queensland University Of Technology, (2006).
[40] J. Bardeen, F.J. Blatt, L.H. Hall, Photoconductivity Conference, Wiley, New York, 1956, p. 146.